

Evaluation of Pseudo-Hepatic Anisotropy Artifact in Liver Intravoxel Incoherent Motion (IVIM) based on Clustering Technique

Oi Lei Wong^{1,2}, Gladys Goh Lo³, Jing Yuan⁴, Wai Kit Chung³, Max W. K. Law⁴, Benny W. H. Ho³, and Michael D. Noseworthy^{2,5}

¹Department of Medical Physics and Applied Radiation Science, McMaster University, Hamilton, Ontario, Canada, ²Imaging Research Center, St.Joseph's Healthcare, Hamilton, Ontario, Canada, ³Department of Diagnostic & Interventional Radiology, Hong Kong Sanatorium & Hospital, Hong Kong, China, ⁴Medical Physics and Research Department, Hong Kong Sanatorium & Hospital, Hong Kong, China, ⁵Department of Electrical and Computer Engineering, McMaster University, Hamilton, Ontario, Canada

Target Audience Researchers and clinicians interested in human body diffusion

Purpose: Non-linear liver motion has been related to pseudo hepatic anisotropy artifact [1]. Although motion correction in IVIM using non-rigid image registration has recently been proposed [2], validation of non-linear motion correction is often challenging [3]. A better understanding on the relationship between pseudo-hepatic anisotropy artifact to IVIM metrics is, therefore, necessary to improve our current approach in IVIM metrics estimation. In this study, we assume the pseudo-hepatic anisotropy artifact affects perfusion related IVIM metrics and gives rise to motion contaminated liver parenchyma. Generally 3 groups of tissues, liver parenchyma, vessels and motion contaminated liver parenchyma, should be present in the liver. Based on this assumption, we hypothesized that the pseudo-hepatic anisotropy artifact can be minimized using multiple diffusion encoding directions.

Material and Methods: Liver imaging was performed on 8 healthy volunteers using a 1.5T MRI (Optima MR450w, General Electric Healthcare, Milwaukee) and a dedicated 32 channel phase array. A non-elastic belt was placed over the volunteer to minimize extensive respiratory motion during free breathing. Coronal diffusion scans (TE/TR=77/2200ms, 5 x 10mm slices, 35cm FOV) were performed with either 1 (along LR, NEX=6) or 6 directions (NEX=1) and b-values of 0, 10, 20, 30, 40, 50, 100, 200, 300, 400, 500 s/mm². Bulk respiratory motion was first corrected with a rigid body transformation using MCFLIRT (FSL, FMRIB, Oxford, UK). Then all NEX were summed before analysis. Voxel-based IVIM analysis was then performed using a custom Matlab script (v.2010a, Mathworks Natick, MA) and a Levenberg-Marquardt Algorithm. Outlier voxels were first identified and excluded based on (1) $f > 1$, $f < 0$, or (2) $D^* < D$, $D^* > 1$ mm²/s. Then cluster analysis based on a 4-dimensional Gaussian mixture model, using IVIM metrics, diffusion, pseudo-diffusion and perfusion fraction (D , D^* and f) and residual sum of squares, was performed over the whole liver. Since the pseudo-hepatic anisotropy artifact was assumed to be perfusion related, the resultant clusters for each subject were then sorted according to their f values. Percent number of voxels within each cluster over the total number of voxels in the whole liver ROI (Percent volume fraction) was calculated for each volunteer. A sign-rank test was performed on each cluster group to compare IVIM metrics and percentage volume fraction calculated using 1 and 6 diffusion encoding directions.

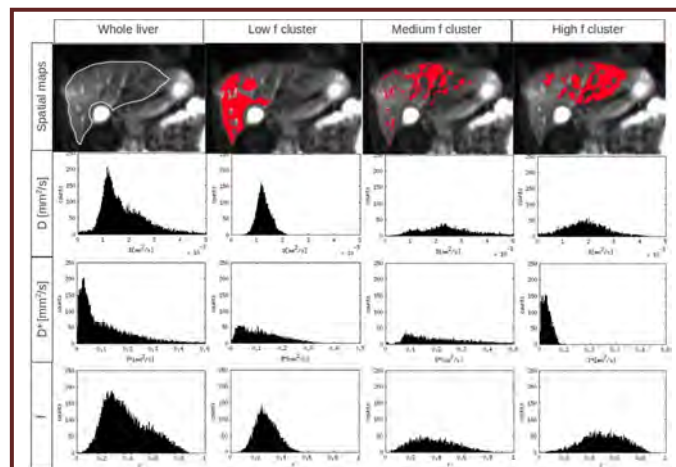


Figure 1: histogram of whole liver, high f, medium f and low f clusters and their corresponding spatial distribution of the same volunteer

| Gradient direction | Clusters | f median (min,max) | $D^* \times 10^{-3}$ mm ² /s median (min,max) | $D \times 10^{-3}$ mm ² /s median (min,max) | Percent Volume Fraction Mean \pm SD |
|--------------------|-------------|-------------------------|---|---|--|
| 1 dir | low f | 0.25 (0.18, 0.28)* | 67.3 (16.2, 133.5) | 1.21 (1.11, 1.57)* | 30 \pm 7 |
| | med f | 0.30 (0.24, 0.38)* | 154.5 (11.9, 209.0) | 1.82 (1.11, 3.01)* | 22 \pm 10 |
| | high f | 0.44 (0.34, 0.60)** | 39.4 (12.9, 145.4) | 1.87 (1.05, 2.68)* | 27 \pm 7 |
| | outlier | 0.18 (0.15, 0.27)* | 1598.8 (1478.1, 2229.5)* | 1.79 (1.67, 2.64)* | 21 \pm 11 |
| 6 dir | whole liver | 0.28 (0.21, 0.34)* | 95.7 (24.9, 157.4) | 1.46 (1.30, 2.02)* | 100 |
| | low f | 0.24 (0.18, 0.29)* | 64.0 (20.0, 133.7) | 1.21 (0.98, 1.76)* | 36 \pm 7 |
| | med f | 0.31 (0.23, 0.40)* | 150.9 (22.7, 100.3)* | 2.12 (1.24, 2.95)* | 23 \pm 8 |
| | high f | 0.41 (0.34, 0.51)** | 37.4 (20.7, 100.3)* | 1.62 (1.19, 2.00)* | 27 \pm 5 |
| | outlier | 0.21 (0.09, 0.33)* | 1515.1 (1347.8, 2964.0)* | 1.83 (1.59, 2.51)* | 14 \pm 8 |
| | whole liver | 0.28 (0.22, 0.37)* | 68.2 (24.6, 126.8) | 1.39 (1.17, 1.97)* | 100 |

Table 1 IVIM metrics (f , D^* , D) and percent volume fraction for each group of cluster using 1 and 6 gradient directional IVIM scans. * indicates significantly different from whole liver, # denotes significant difference compared to low f cluster, & denotes significant different from medium f cluster. ♦ denotes significant difference between 1 and 6 gradient directions (all comparisons made with $P < 0.05$ level of significance).

reduced D^* with the high f cluster was also observed in 6 direction scans.

Discussion: Motion contaminated parenchyma has previously been observed in the left liver lobe, where prominent pseudo-hepatic diffusion artifact has been identified [1]. The observed spatial association between left liver lobe and high f cluster in this study, thus, supported our assumption. Since the pseudo-hepatic anisotropy artifact is directional, use of 6 non-coplanar gradient directions leads to the observed D^* reduction in high f clusters (hypothesized to motion contaminated liver parenchyma). More importantly, the observed decrease in outliers and increase in percent low f cluster volume fraction shows better IVIM fit using more gradient directions.

Conclusion: Pseudo-hepatic anisotropy artifact was minimized by acquiring multiple non-coplanar diffusion encoding directions. The observed spatial distribution of high f cluster also supports our assumption that pseudo-hepatic anisotropy artifact affects the perfusion related IVIM metrics.

References: [1] Nasu et al. MAGMA. 2007;20:205-11; [2] Mazaheri et al. Acad Radiol. 2012;19:1573-80; [3] Murphy et al. MRM. 2013;70:1460-9;